Available online at www.sciencedirect.com
SCIENCE DIRECT®
International Journal of Multiphase Flow 30 (2004) 89–103
International Journal of Multiphase Flow
www.elsevier.com/locate/ijmulflow

What is entrainment in vertical two-phase churn flow?

B.J. Azzopardi *, E. Wren

Multiphase Flow Research Group, Nottingham Fuel and Energy Centre, School of Chemical, Environmental and Mining Engineering, University of Nottingham, University Park, Nottingham NG7 2RD, UK

Received 6 October 2002; received in revised form 11 May 2003

Abstract

Churn flow, the least understood of the flow patterns in vertical upflow in pipes, has been receiving attention recently. One particular aspect addressed is the fraction of liquid entrained in the gas phase. This paper reports on how data on the phase split at T-junctions has been used to determine this fraction at liquid flow rates much higher than hitherto. The results and other available data are examined to question whether the entrained liquid is being carried as drops or travelling in huge waves which have been identified as being present at the flow rates corresponding to churn flow.

Keywords: Gas/liquid; Vertical; Churn flow; Entrainment

1. Introduction

When considering the flow of a gas/liquid mixture in pipes most researchers group the wide variety of ways in which the phases can distribute themselves about the pipe cross-section by describing the features through a limited number of flow patterns. These encapsulate the main features of the flow. Though many names and descriptions have been identified, there is now a consensus to stick to a well defined set of names, e.g., for upflow in a vertical pipe these are taken as bubbly, slug, churn and annular. There is a reasonable amount of information for bubble, slug and annular flow, though models for these are not yet universally applicable. Churn flow is much less understood.

There is a modicum of consensus on the mechanisms causing transitions between flow patterns to occur. Initially the bubble/slug transition was considered to occur by coalescence of bubbles.

* Corresponding author. Tel.: +44-115-951-4160; fax: +44-115-951-4115.
E-mail address: barry.azzopardi@nottingham.ac.uk (B.J. Azzopardi).

0301-9322/$ - see front matter
doi:10.1016/j.ijmultiphaseflow.2003.11.001

The frequency of collision was determined to depend on void fraction, increasing rapidly beyond values of 0.25–0.3. This, together with the buoyancy driven bubble rise velocity, can be used to determine a flow pattern boundary criterion. However, this concept does not explain why the coalescence occurs at regular intervals to produce the approximately evenly spaced, large Taylor bubbles that characterise slug flow. More recent ideas have focussed on the waves of bubble concentration that are found in bubbly flow. The high concentration points will give local occurrences of coalescence. Interestingly, the velocity of these void fraction waves have been found to have the same relationship with mixture velocity as do the Taylor bubbles in slug flow, (Cheng et al., 1998). As yet there is no mathematical description for this approach. It is noted that slug flow has not been observed in larger diameter pipes. The maximum diameter at which Taylor bubbles have been seen is less than 0.1 m. Kytömaa and Brennen (1991) who experimented on a 0.102 m diameter pipe found that the transition was from bubble to churn-turbulent rather than slug flow. Lammers and Biesheuvel (1996) reported that bubble to slug did occur in a 0.08 m diameter pipe.

For the slug/churn transition one proposal is that growth of waves on the liquid film surrounding Taylor bubbles can lead to local flooding. Jayanti and Hewitt (1992) and Watson and Hewitt (1999) developed a model based on these ideas that gives good predictions of experimental data including the effect of system pressure. In contrast, Mishima and Ishii (1984) and Brauner and Barnea (1986) have presented a model based on excessive bubble entrainment into the liquid slug and its subsequent break down.

The churn/annular transition has been related to the flow reversal phenomena for smaller diameter pipes. In larger diameter pipes the transition is considered to depend on the drops being carried up. This normally depends on drop size. The model of Taitel et al. (1980) specifies this drop size as the maximum size that can survive without undergoing aerodynamic breakup. The resulting transition criterion is a dimensionless superficial gas velocity, the Kutateladze number. The transition is considered independent of liquid flow rate. For higher liquid flow rates, Barnea (1986) proposed an alternative mechanism. This considered that when films were thick enough they might have a void fraction similar to that of the bubbly liquid slugs. The film might become unstable and transform into the bubbly flow. She developed equations to describe this transition. It shows the correct trends but there is very little data in this region.

2. Churn flow

Part of the confusion about churn flow has been attributed by Barbosa et al. (2001a) to the fact that the word churn has been employed for a number of flow types, i.e., Zuber and Findlay (1965) used it as churn-turbulent to describe what they considered to be type of bubbly flow; Taitel et al. (1980) considered churn flow to be a developing slug flow and Hewitt and Hall-Taylor (1970) used it to define the region intermediate between slug and annular flows. Here, available literature is examined to understand the nature of churn flow and the flow rates over which it occurs.

The ranges of flow rates that cover churn flow have been studied recently by a number of groups (Sekoguchi and Mori, 1997; Furukawa and Fukano, 2001; Sawai and Kaji, 2001) utilising modern instrumentation that reveals the structure of the flow. One method uses conductance probes regularly spaced along the test section to obtain cross-section averaged void fractions.

Examination of the space/time information shows much detail. In addition, Sekoguchi and Mori (1997) also used an array of 67-needle probes facing upstream mounted across a diameter. These were mounted in electrical circuits and could determine whether the needle tip was in air or water. In all cases the second electrode is the pipe wall or the metal strap supporting the needles. As the needles were sampled simultaneously, the liquid profile across a diameter was obtained. In the region beyond bubbly flow they reported three major enduring structures: slugs, huge waves and disturbance waves. Slugs filled the pipe cross-section and travelled at velocities well predicted by the equation of Nicklin and Davidson (1962). Huge waves were distinguished in having an almost linear relationship between velocity and width. They had velocities larger than disturbance waves but lower than those of slugs. Disturbance waves, which occurred at higher gas and lower liquid velocities, had a much lower dependence of velocity on wave width. The width velocity relationship can be described by a power law with an exponent of about 0.25. At low liquid flow rates, the frequency of disturbance waves was found by many workers to increase with increasing liquid flow rate (Azzopardi, 1997). The data of Sekoguchi and Mori (1997) follows this trend up to liquid superficial velocities $\approx$0.25 m/s. Thereafter, the frequency decreases with increasing liquid flow rate. No other study has worked at such high flow rates. Disturbance wave velocities increase with both gas and liquid flow rates with power law exponents of 0.25 and 0.4 respectively.

Sekoguchi and Mori (1997) reported that more than one of the above structures could be present at a particular combination of flow rates with specific structures being more dominant depending on the flow rates studied. They defined transitions at which the frequencies of occurrence of slugs and huge waves and of huge waves and disturbance waves were equal. Fig. 1 shows the position of these boundaries on a flow pattern map together with the transition lines from the map of Hewitt and Roberts (1969) and those based on models of transition from Taitel et al. (1980) (bubble/slug), Brauner and Barnea (1986) (slug/churn, Sl Ch) and Kaya et al. (2000) (intermittent/annular). It can be seen that the huge wave/disturbance wave boundary is similar to the intermittent/annular boundary (as well as the alternating phases/gas continuous boundary of Duns and Ros (1963) which are not shown here) at very low liquid flow rates. At higher flow rates

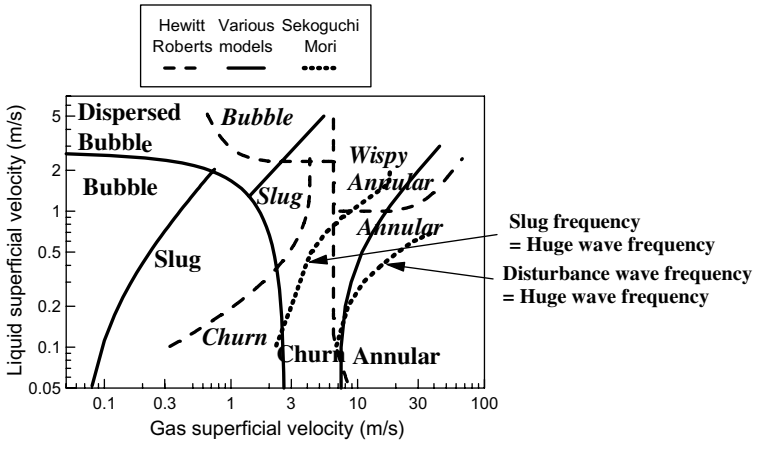

Fig. 1. Composite flow pattern map showing boundaries proposed by several papers. Italic flow pattern names refer to flow pattern map of Hewitt and Roberts (1969).

it moves to higher gas flow rates as the liquid flow rate increases as do the curves of Kaya et al. and that of Duns and Ros.

Recent observations of churn flow have begun to give a clearer, less vague description than previously. From their work with photochromic dyes, Hewitt et al. (1985) reported that the waves transport liquid upwards whilst the base film between them flows downwards under gravity. Total pressure drop and void fraction have been measured in this region. For the latter, Barbosa et al. (2001a) report work with quick closing valves whilst Sawai and Kaji (2001) used their conductance probes to obtain averaged void fractions. When they used the void fractions to determine the gravitational pressure drop and by difference the frictional pressure drop they found that this quantity was negative for lower gas superficial velocities. Sawai and Kaji show that the transition between positive and negative values of frictional pressure drop moved to lower gas velocities as the liquid flow rate was increased. Their data for a liquid superficial velocity of 0.2 m/s showed only positive values of frictional pressure drop.

Barbosa et al. (2001b) have developed a model of the waves in churn flow. They assumed that the waves were of sinusoidal shape, preferring this to the semicircular shape suggested by McQuillan et al. (1985) and the asymmetric shape used for flooding by Shearer and Davidson (1965), noting that it was a reasonable approximation to the shapes found in the work of Hewitt et al. (1985). They discuss the creation of waves at the porous wall inlet for the liquid. Thereafter, the waves are taken to travel upward with a downwards-falling film in between. The thickness of the falling film was calculated using the classical equation of Nusselt (1915). A force balance was then constructed over the wave involving forces due to gravity, pressure on the gas core, pressure on the liquid, wall shear and interfacial shear. The pressure variation in the core is determined from a Bernoulli analysis on the gas phase and an assumption of flow separation downstream of the crest—this implies constant pressure of the downstream part of the wave. The sum of forces was used to determine the acceleration of the waves using Newton's second law of motion. This results in predictions of wave velocities. However, these tend to have much higher values than those measured. Sawai and Kaji (2001) considered that the frictional pressure drop in churn flow to be dominated by the waves. This requires wave velocities, which they indicated could be determined from a void fraction wave analysis.

3. Entrained fraction

One facet of churn flow that has received attention recently is the amount of liquid carried in the centre of the channel. Published material assumes that this liquid is carried as drops. Data for the fraction of liquid so carried, usually termed the entrained fraction, has been reported by Wallis (1962), Verbeek et al. (1992), Fore and Dukler (1995), Azzopardi and Zaidi (2000) and Barbosa et al. (2002). The information shows that, unlike in the annular flow region where entrained fraction increases with gas flow rate, in churn flow entrained fraction decreases with increasing gas superficial velocity. Fig. 2 shows data from three different pipe diameters. Those from the small diameter pipe, Azzopardi and Zaidi (2000), are for a superficial liquid velocity of 0.08 m/s. The data in the other two diameters, Verbeek et al. (1992), are from liquid superficial velocities of 0.013 and 0.01 m/s respectively. Also shown, as open symbols, are the values of minimum entrained fraction calculated from the equation developed by Barbosa et al. and given as Eq. (1)

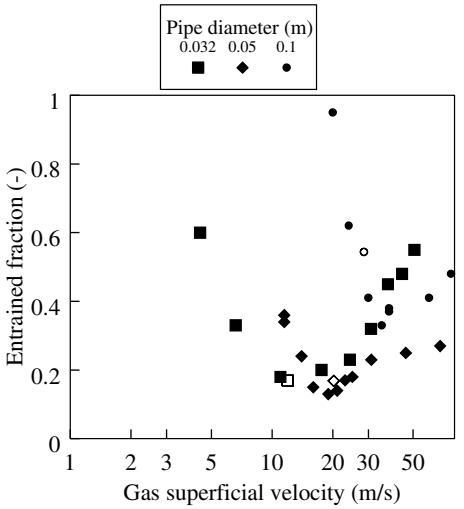

Fig. 2. Effect of gas superficial velocity on entrained fraction showing different trend in churn flow region. Open symbols are minimum entrained fraction values calculated using equation of Barbosa et al. (2002).

$$E_{fT} = 3.4255 D_t^2 \sqrt{\frac{\rho_L \dot{m}_L}{\rho_G \dot{m}_G}} + 0.0095 \tag{1}$$

This minimum is taken to occur at the transition to annular flow, i.e., at a dimensionless gas velocity of $u_G^* = \frac{\dot{m}_G}{\sqrt{\rho_G(\rho_L - \rho_G) g D_t}} = 1$. Here $\dot{m}_G$ and $\dot{m}_L$ are the mass fluxes of gas and liquid, ρ_G, ρ_L are the densities of the gas and liquid, g is the gravitational acceleration and D_t is the pipe diameter.

It is instructive to consider the methods employed to determine entrained fraction. Wallis (1962) used a concentric pipe arrangement to separate the core and wall flows. Barbosa et al. (2002) used a sampling probe of 0.00625 m in a 0.032 m diameter pipe. Measurements were taken at the centre line and 0.2 pipe diameters on either side. Other researchers determined entrained fraction from measurements of film flow rates obtained with a slot or porous wall device. In both cases the basis of the method is to suck off all of the film with the minimum amount of gas. To ensure that this is achieved, the test is repeated with increasing take off whilst the flow rates of gas and liquid taken off are measured at each stage. A plot of the flow rate of liquid taken off against that of the gas shows a plateau, which can be taken as the film flow rate. However, Azzopardi and Zaidi (2000) have reported an anomalous behaviour in the churn flow region. Here there is a tendency for liquid take off to increase with gas take off between the liquid only region and the plateau. Two values of film flow rate might be deduced. One corresponds to the plateau, the other to the first take off of gas. It is the latter that has been used to produce the churn flow data in Fig. 2.

4. Use of T-junction data

In annular flow, the maldistribution of the phases that occurs at a T-junction with a vertical main pipe and a horizontal side arm has been attributed to the different momentum fluxes of the

film, the gas and the drops. It is argued that the fluids with the lower momentum fluxes will be most easily diverted into the side arm. For typical low pressure conditions the momentum fluxes of the gas and liquid are similar and much lower than that of the drops. Therefore, gas and film will be diverted. From information on the behaviour of single phase flow at junctions, it is expected that fluid from the segment of main pipe nearest the side arm will be taken off with the chord defining the segment moving further from the side arm with increasing take off. If applied to annular flow, this observation results in the following equation to describe the phase maldistribution.

$$\frac{\dot{M}_{G3}}{\dot{M}_{G1}} = \frac{1}{2\pi}\left[\left(\frac{2\pi}{\{1-E_f\}K}\frac{\dot{M}_{L3}}{\dot{M}_{L1}}\right) - \sin\left(\frac{2\pi}{\{1-E_f\}K}\frac{\dot{M}_{L3}}{\dot{M}_{L1}}\right)\right] \tag{2}$$

Here, $\dot{M}_G$ and $\dot{M}_L$ are the mass flow rates of the gas and liquid, respectively, and the subscripts 1 and 3 refer to the main pipe and side arm, respectively. E_f is the entrained fraction and K is a factor to allow for the effect of side arm to main pipe diameters. Azzopardi (1984) showed that for equal diameter junctions this is equal to 1.2. The deviation from 1.0 is probably due to the dividing boundaries between fluid being taken off or not being curved concavely, rather than being chords, as observed by Charron and Whalley (1995). Eq. (2) has been shown to give good predictions of phase split when no other mechanisms were occurring.

In churn flow the same equation might apply if there is entrainment and a wall film. Indeed, if the phase split were known, the equation could be utilised to back out the entrained fraction. Azzopardi (1999) identifies sources of phase split data at junctions with vertical main pipes. Those which give data from the churn flow region at low take off are summarised in Table 1. Data from these sources have been used to back out the entrained fraction using Eq. (2). Fig. 3 shows an example of the goodness of fit. The conditions at which the experiments of Zetzmann (1984) were carried out are shown on Fig. 4. The flow patterns reported were slug, churn and annular. This agrees with the flow patterns predicted using the transition criteria of Taitel et al. (1980) for bubble/slug, that of Brauner and Barnea (1986) for dispersed bubble/slug/churn and that of Kaya et al. (2000) for the transition to annular flow. It is surprising that there is slug flow reported in the 0.1 m diameter pipe. Other sources have indicated that slug flow does not occur in such large diameters (Kytömaa and Brennen, 1991; Cheng et al., 1998).

The entrained fractions determined from the above approach are shown in Figs. 5–10. Fig. 5 shows data determined from the experiments of Zetzmann (1984) for a constant liquid superficial velocity. This shows only a very small effect of gas velocity for values above 3.5 m/s and no variation of pipe diameter over the fourfold range in diameter. Data from the 0.024 m diameter pipes

Table 1
Details of sources of phase split data for vertical flow patterns other than annular

Sources	Inlet diameter (m)	Diameter ratio	Pressure (bar)	Gas superficial velocity (m/s)	Liquid superficial velocity (m/s)
Zetzmann (1984)	0.024, 0.05, 0.1	0.5, 1.0	2	0.2–48	0.5–2.5
Hewitt et al. (1990)	0.032	0.6, 1.0	3–4.4	2.2–11.7	0.8–2.4
Azzopardi et al. (submitted for publication)	0.07	1.0	1	1.1–11.8	0.02–1.83

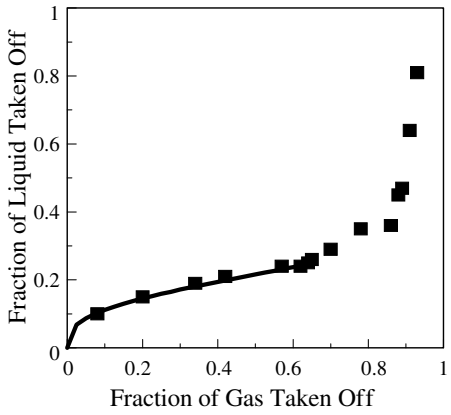

Fig. 3. Examples of goodness of fit in backing out values of entrained fraction: diameter = 0.076 m, pressure = atmospheric, gas superficial velocity = 10 m/s, liquid superficial velocity = 0.8 m/s.

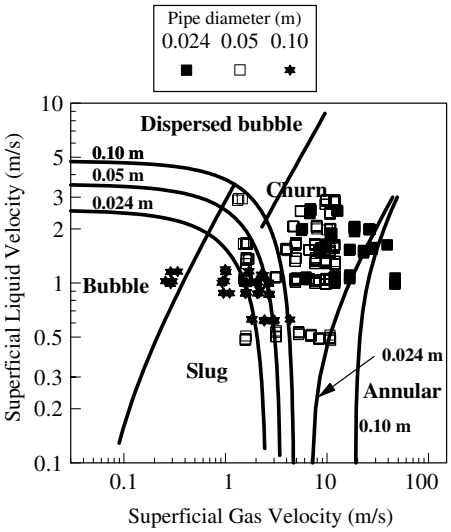

Fig. 4. Flow pattern map showing conditions at which data was taken by Zetzmann (1984). Transition lines are calculated using models of Taitel et al. (1980) (bubble/slug and bubble/dispersed bubble), Brauner and Barnea (1986) (slug/churn) and Kaya et al. (2000) (intermittent/annular).

shows a small but systematic effect of liquid flow rate (Fig. 6). This is seen more clearly in the in the expanded plot (Fig. 7). A similar trend is seen in the data from the 0.05 m diameter pipe (Fig. 8).

Figs. 9 and 10 show equivalent data from the experiments reported by Hewitt et al. (1990) and Azzopardi et al. (submitted for publication). The same trends as noted above for the data of Zetzmann (1984) are present. However, there is more scatter and data are available at fewer gas velocities. Part of the scatter might be attributed to the hysteresis reported by Azzopardi et al. (submitted for publication); slightly different take off values were recorded according to whether the fractional take off was being increased or decreased.

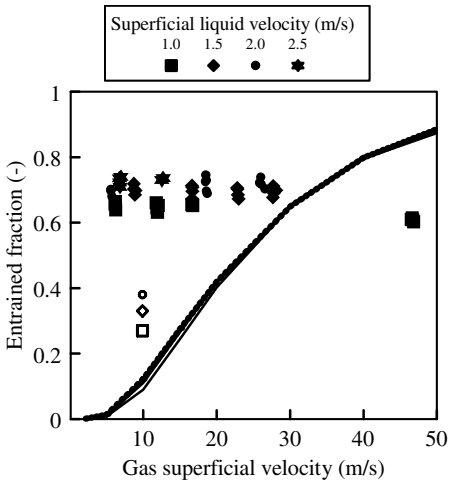

Fig. 5. Entrained fraction determined from the T-junction data of Zetzmann (1984). Inlet liquid superficial velocity = 1 m/s. Open symbols are minimum entrained fraction values predicted by equation of Barbosa et al. (2002). Lines are predictions of annular flow model of Hewitt and Govan (1990).

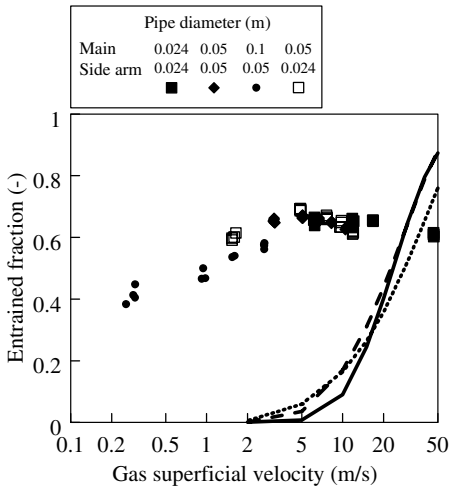

Fig. 6. Effect of phase superficial velocities on entrained fraction determined from the T-junction data of Zetzmann (1984). Pipe diameter = 0.024 m. Lines are predictions of annular flow model of Hewitt and Govan (1990).

Consideration has been given to the uncertainty in the estimation of entrained fraction from the above data. Azzopardi et al. (submitted for publication) report the greatest uncertainties arose from mass balances across the three legs of the junction. They found that most data has mass balance differences of within 3% for the liquid and 6% for the gas. Because of the shape of the curve being fitted and illustrated in Fig. 3, the uncertainty in the liquid measurement corresponds to a maximum uncertainty in entrained fraction of 5%. The shape of the curve in Fig. 3 indicated that the uncertainty effect of gas phase measurements is smaller. This level of uncertainty is equal

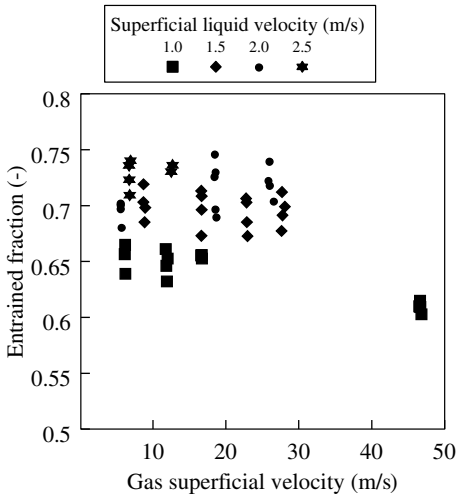

Fig. 7. Effect of phase superficial velocities on entrained fraction determined from the T-junction data of Zetzmann (1984). Expanded scale. Pipe diameter = 0.024 m.

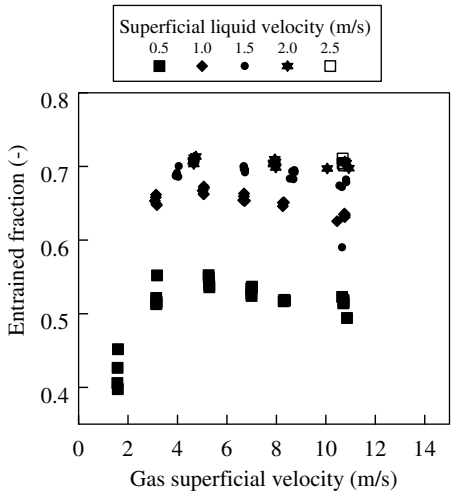

Fig. 8. Effect of phase superficial velocities on entrained fraction determined from the T-junction data of Zetzmann (1984). Expanded scale. Pipe diameter = 0.05 m.

to or less than those for measurements of entrained fraction using other techniques as discussed by Azzopardi and Zaidi (2000).

5. Discussion

The entrained fraction data shown in Figs. 5–10 show no effect of pipe diameter, little trend with superficial gas velocity for velocities greater than 5 m/s, and a small but significant trend with liquid superficial velocity. A simple dimensional equation has been developed to describe the data.

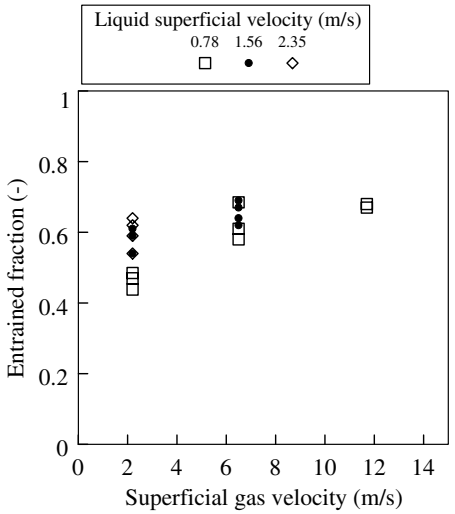

Fig. 9. Entrained fraction determined from the T-junction data of Hewitt et al. (1990).

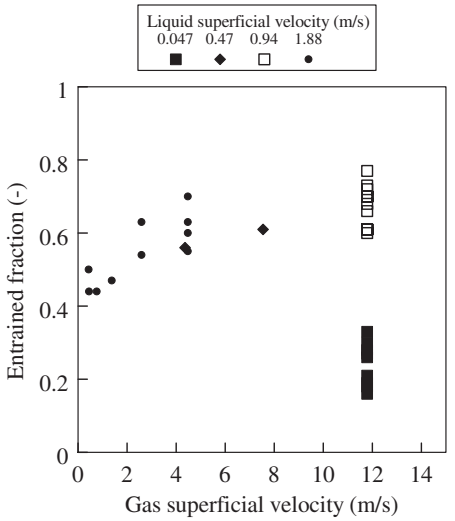

Fig. 10. Entrained fraction determined from the T-junction data of Azzopardi et al. (submitted for publication).

$$E_f = 0.47 u_{gs}^{0.16} u_{ls}^{0.35} \quad \text{for } u_{gs} < 5 \text{ m/s}$$
$$E_f = 0.6 u_{ls}^{0.35} \quad \text{for } u_{gs} > 5 \text{ m/s} \tag{3}$$

The accuracy of the predictions using this equation for the low gas, high liquid inlet conditions of churn flow is shown in Fig. 11. Due to the lack of experimental data collected for these relevant situations, the predicted entrained fraction is shown against the entrained fraction deduced from the known phase split data at a vertical T-junction using Eq. (2). This has a mean error of 3% and

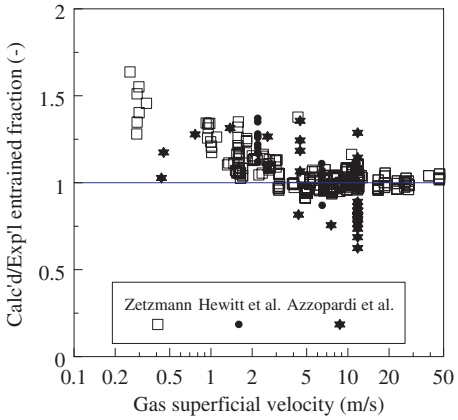

Fig. 11. Accuracy of simple correlation proposed for entrained fraction—Eq. (3).

a standard deviation of 11.7%. It is noted that all data considered were obtained with air/water mixtures at pressures of 1–3 bar.

The entrained fractions obtained here have been compared with those predicted by the annular flow model of Hewitt and Govan (1990). As seen in Figs. 5 and 6, the predictions show the trend that is expected for annular flow, entrained fraction increasing as the gas velocity increases. This is different to the present data which appears almost constant for gas superficial velocities >5 m/s. The minimum values of entrained fraction at the churn/annular boundary from equation of Barbosa et al. (2002) are shown in Fig. 6 (open symbols). These underpredict. It is noted that the databases used to derive the equations for the rates of entrainment and deposition used in the model of Hewitt and Govan (1990) and the equation of Barbosa et al. (2002) have hardly any points with the high liquid superficial velocities of the present data.

The basis of the division of phases at T-junctions is the difference in momentum flux of the different parts of the liquid. In annular flow, these are the film and the drops. However, can the same be said to be correct for churn flow? It has been noted that churn flow has been described as waves moving upwards with a falling film in between. The area of churn flow overlaps that for huge waves as defined by Sekoguchi and Mori (1997). If the momentum flux of the huge waves is compared to that of the gas, it can be seen that the ratio is very large (Fig. 12). In contrast, the momentum flux of the film will be around zero. Therefore, it is possible that the film is taken off and the waves carry straight on, i.e., the entrained fraction is the fraction of liquid travelling in the huge waves as well as a part travelling as drops. The predictions of Eq. (3) have also been compared with entrained fraction data obtained by Barbosa et al. (2002) around the churn/annular flow pattern transition. They obtained entrained fraction data from measurements of drop fluxes across the pipe diameter. They show the entrained fraction to be fairly independent of gas velocity over the range of dimensionless gas velocities of 0.9–1.5. The entrained fraction increases at lower gas velocities. The data at the lowest gas velocity lies around the predictions of Eq. (3), though there is considerable scatter. The minimum values at dimensionless gas velocities around 1.0 are lower than those given by Eq. (3).

Examination of the composite flow pattern map, Fig. 1, shows that the huge wave region extends over both the churn flow and wispy annular flow regions. It is sensible to ask if wisps are

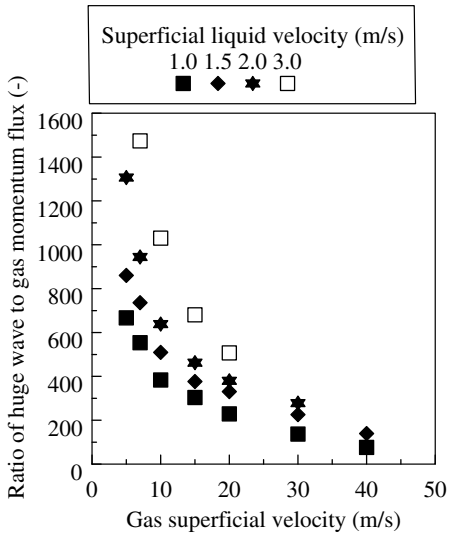

Fig. 12. Ratio of momentum flux for huge wave to that for the gas calculated from the data of Sekoguchi and Mori (1997).

the same as huge waves. Bennett et al. (1965) were the first to report on wispy annular flow. They identify it as having "a continuous relatively slow moving liquid film on the tube walls and a more rapidly moving entrained phase in the gas core". The latter they describe as, "This phase appeared to flow in large agglomerates somewhat resembling ectoplasm". Flash photography only revealed bubbles near the transparent pipe wall. X-ray photographs showed what appeared to be a filament of material in the core, a filament of apparently gas rich froth in the process of breaking down. Sekoguchi and Mori (1997) used their instrumentation at conditions well into the wispy annular region on the flow pattern map of Hewitt and Roberts (1969). They present data from their 67-needle probe array which show large aerated structures, presumably huge waves, but no large liquid agglomerates in the core. Prasser et al. (2001) used a mesh electrode technique. This has two grids of 16 electrodes each stretched at 3 mm intervals along chords. The second grid is 1.5 mm downstream of the first with its wires perpendicular to those of the first grid. They report one case in the wispy annular region of the Hewitt/Roberts map. The wispy structure they present is very similar to the huge waves reported by Sekoguchi and Mori (1997). It can be seen that the frequencies of huge waves and wisps have similar values for the same flow rates (Fig. 13). Here the huge wave data were taken on a 0.026 m diameter pipe (Sekoguchi and Mori, 1997). The wisp frequencies are from Hawkes et al. (2000) (0.032 m) and Prasser et al. (2001) (0.05 m). Hawkes et al. determined the frequency using infrared sources and detectors mounted across a pipe diameter. In the base experiment they obtained a power spectrum with two peaks with frequencies of about 5 and 15 Hz. When the experiment was repeated with part of the liquid sucked off through a porous wall section, the spectrum was seen to one contain the 5 Hz peak. Fig. 13 shows the range of frequencies reported by Hawkes. The higher frequency corresponds to that expected for disturbance waves. The lower frequency peak was identified as being from wisps. This agreement of frequencies for the two phenomena could, of course, be a coincidence. However, it could also be evidence of the sameness of huge waves and wisps.

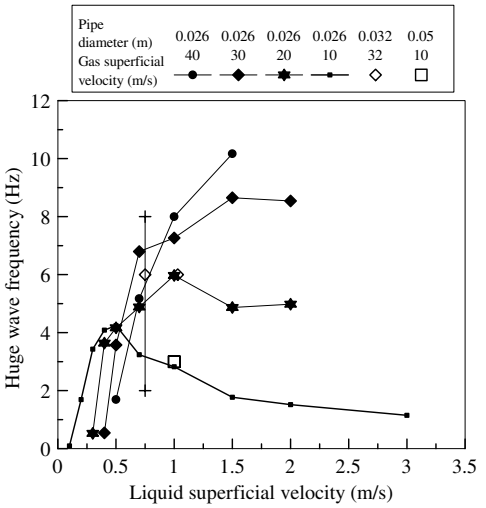

Fig. 13. Frequency of huge waves and wisps. Data from 0.026 m diameter pipe is from Sekoguchi and Mori (1997), that from the 0.032 m diameter pipe from Hawkes et al. (2000) and that from the 0.05 m diameter pipe from Prasser et al. (2001). Closed symbols indicate huge waves and open symbols wisps. The crosses mark the limits of the range of data for the 0.032 m diameter data.

The results of the experiments where the film is sucked off through a porous wall section reported by Azzopardi and Zaidi (2000) can be interpreted as giving a measure of the momentum of different parts of the liquid. For annular flow, there is initially just liquid taken off. This is followed by a plateau with no increase in the liquid taken off. Further take off of liquid only occurs when a very significant portion of the gas is taken off. This can be interpreted as firstly film being taken off and then drops. For churn flow there is an extra region. Like in annular flow, there is an initial region where there is just liquid is taken off. This is followed by a region of increasing liquid take off with augmenting gas take off, and then a plateau. This probably indicates a base film that is easily taken off followed by suck off of fast moving waves, which are difficult to extract. The measurements of Sekoguchi and Mori (1997) show that the predominant waves in this region, huge waves, have velocities that come close to those of the gas.

The three-part take off from churn flow is also seen in data reported by Assad et al. (1998) for inlet conditions which lie in the wispy annular flow region when plotted on the flow pattern map of Hewitt and Roberts (1969). Analysis of the information from Assad et al. suggests that 7% of the liquid is in the base film, 71% in the huge waves and 22% in drop form.

6. Conclusions

From the above it can be concluded that:

- Vertical churn flow can be described as huge waves moving upwards with a falling film in between and a small amount of liquid droplets carried in the centre of the channel. The area

of occurrence of huge waves covers the conventional churn flow and wispy annular flow patterns.

- The entrained fraction as estimated from data on phase split at T-junctions in churn flow shows little effect of pipe diameter or inlet gas superficial velocity. There is a stronger effect of liquid flow rate, particularly at low flow rates. Entrained fraction is seen to increase with increasing liquid velocity. For the split of churn flow at a T-junction it was found that the (lower momentum) base film was easily extracted but the huge waves were found to have a similar momentum to the gas core and thus not diverted into the branch arm. A simple description of entrained fraction for churn flow has been developed. This uses separate equations for high and low gas velocities. It has an average error of 3% with a standard deviation of 11.7%.
- It appears that much of the entrained liquid in churn flow is carried in huge waves. It is not clear what wisps are. Might it be possible that they are highly aerated huge waves?
- The frequency of the huge waves were found to be very similar to the frequency of wisps found in wispy annular flow.

References

Assad, A., Jan, C., Lopez de Bertodano, M., Beus, S., 1998. Scaled experiments in ripple annular flow in a small tube. Nucl. Eng. Des. 184, 437–447.

Azzopardi, B.J., 1984. The effect of side arm diameter on two phase flow split at a T junction. Int. J. Multiphase Flow 10, 509–512.

Azzopardi, B.J., 1997. Drops in annular two-phase flow. Int. J. Multiphase Flow 24, S1–S53.

Azzopardi, B.J., 1999. Phase split at T-junctions. Multiphase Sci. Technol. 11, 223–329.

Azzopardi, B.J., Zaidi, S.H., 2000. Determination of entrained fraction in vertical annular gas/liquid flow. J. Fluids Eng. 122, 146–150.

Azzopardi, B.J., Conte, G., Wren, E. The split of slug/churn flow at a vertical T-junction, submitted for publication.

Barbosa, J., Richardson, S., Hewitt, G.F., 2001a. Churn flow: myth, magic and mystery. In: 39th European Two-Phase Flow Group Meeting, Aveiro, Portugal, 18–20 June.

Barbosa, J., Govan, A.H., Hewitt, G.F., 2001b. Visualisation and modelling studies of churn flow in a vertical pipe. Int. J. Multiphase Flow 27, 2105–2127.

Barbosa, J.R., Hewitt, G.F., König, G., Richardson, S.M., 2002. Liquid entrainment, droplet concentration and pressure gradient at the onset of annular flow in a vertical pipe. Int. J. Multiphase Flow 28, 943–961.

Barnea, D., 1986. Transition from annular flow and from dispersed bubble flow—unified models for the whole range of pipe inclinations. Int. J. Multiphase Flow 12, 733–744.

Bennett, A.W., Hewitt, G.F., Kearsey, H.A., Keeys, R.K.F., Lacey, P.M.C., 1965. Flow visualisation studies of flow boiling at high pressures. Proc. Inst. Mech. Eng. 180 (Part 3C), 1–11.

Brauner, N., Barnea, D., 1986. Slug/churn transition in upward gas–liquid flow. Chem. Eng. Sci. 41, 159–163.

Charron, Y., Whalley, P.B., 1995. Gas–liquid annular flow at a vertical tee junction—part I. Flow separation. Int. J. Multiphase Flow 21, 569–589.

Cheng, H., Hills, J.H., Azzopardi, B.J., 1998. A study of the bubble-to-slug transition in vertical gas–liquid flow in columns of different diameters. Int. J. Multiphase Flow 24, 431–452.

Duns, H., Ros, N.C.J., 1963. Vertical flow of gas and liquid mixtures in wells. In: 6th World Petroleum Congress, Section II, Paper 22-PD6.

Fore, L.B., Dukler, A.E., 1995. Droplet deposition and momentum transfer in annular flow. AlChE J. 41, 2040–2046.

Furukawa, T., Fukano, T., 2001. Effects of liquid viscosity on flow patterns in vertical upward gas–liquid two-phase flow. Int. J. Multiphase Flow 27, 1109–1126.

Hawkes, N.J., Lawrence, C.J., Hewitt, G.F., 2000. Studies of wispy-annular flow using transient pressure gradient and optical measurements. Int. J. Multiphase Flow 26, 1565–1582.

Hewitt, G.F., Govan, A.H., 1990. Phenomenological modelling of non-equilibrium flows with phase change. Int. J. Heat Mass Transfer 33, 229–242.

Hewitt, G.F., Hall-Taylor, N.S., 1970. Annular Gas–Liquid Flow. Pergamon Press, Oxford.

Hewitt, G.F., Roberts, D.N., 1969. Studies of two-phase patterns by simultaneous X-ray and flash photography. UKAEA Report AERE M2159.

Hewitt, G.F., Martin, C.J., Wilkes, N.S., 1985. Experimental and modelling studies of annular flow in the region between flow reversal and the pressure drop minimum. Physiochem. Hydrodyn. 6, 69–86.

Hewitt, G.F., Gill, L.E., Roberts, D.N., Azzopardi, B.J., 1990. The split of low inlet quality gas/liquid flow at a vertical T—Experimental data. UKAEA Report AERE M3801.

Jayanti, S., Hewitt, G.F., 1992. Prediction of slug-to-churn transition in vertical two-phase flow. Int. J. Multiphase Flow 18, 847–860.

Kaya, A.S., Chen, X.T., Sarica, C., Brill, J.P., 2000. Investigation of transition from annular to intermittent flow in pipes. J. Energy Res. Technol. 122, 22–28.

Kytömaa, H.K., Brennen, C.E., 1991. Small amplitude kinematic wave propagation in two-component media. Int. J. Multiphase Flow 17, 13–26.

Lammers, J.H., Biesheuvel, A., 1996. Concentration waves and the instability of bubbly flows. J. Fluid Mech. 328, 67–93.

McQuillan, K.W., Whalley, P.B., Hewitt, G.F., 1985. Flooding in vertical two-phase flow. Int. J. Multiphase Flow 11, 741–760.

Mishima, K., Ishii, M., 1984. Flow regime transition criteria for two-phase flow in vertical tubes. Int. J. Heat Mass Transfer 27, 723–734.

Nicklin, D.J., Davidson, J.F., 1962. The onset of instability in two-phase slug flow. In: Institution Mechanical Engineers Symposium on Two-Phase Flow, London.

Nusselt, W., 1915. Die oberflachenkondensation des wasserdampfes. VDI Z. 60, 541–546, 569–575.

Prasser, H.-M., Krepper, E., Lucas, D., 2001. Fast wire-mesh sensors for gas–liquid flows and decomposition of fraction profiles according to bubble size classes. In: Celata, G.P., Di Marco, P., Goulas, A., Mariani, A. (Eds.), Experimental Heat Transfer, Fluid Mechanics and Thermodynamics 2001, 2. Editzioi ETS, Pisa, pp. 1135–1140.

Sawai, T., Kaji, M., 2001. Flow structure and pressure gradient in churn flow. In: Celata, G.P., Di Marco, P., Goulas, A., Mariani, A. (Eds.), Experimental Heat Transfer, Fluid Mechanics and Thermodynamics 2001, 2. Editzioi ETS, Pisa, pp. 1791–1796.

Sekoguchi, K., Mori, K., 1997. New development of experimental study on interfacial structures in gas–liquid two-phase flow. In: Celata, G.P., Di Marco, P., Goulas, A., Mariani, A. (Eds.), Experimental Heat Transfer, Fluid Mechanics and Thermodynamics 1997, 2. Editzioi ETS, Pisa, pp. 1177–1188.

Shearer, C.J., Davidson, J.F., 1965. The investigation of a standing wave due to gas blowing upwards over a liquid film; its relation to flooding in wetted-wall columns. J. Fluid Mech. 22, 321–335.

Taitel, Y., Barnea, D., Dukler, A.E., 1980. Modelling flow pattern transitions for steady upward gas–liquid flow in vertical tubes. AlChE J. 26, 345–354.

Verbeek, P.H.J., Miesen, R., Schellenkens, C.J., 1992. Liquid entrainment in annular dispersed upflow. In: 8th Annual European Conference on Liquid Atomisation and Spray Systems, Amsterdam, 30 September–2 October, pp. 33–45.

Wallis, G.B., 1962. The onset of droplet entrainment in annular gas–liquid flows. General Electric Report No. 62GL127.

Watson, M.J., Hewitt, G.F., 1999. Pressure effects on the slug to churn transition. Int. J. Multiphase Flow 25, 1225–1241.

Zetzmann, K., 1984. Phase separation of air–water flow in a vertical T-junction. Ger. Chem. Eng. 7, 305–312.

Zuber, N., Findlay, J.A., 1965. Average volumetric concentration in two-phase flow systems. J. Heat Transfer 87, 453–468.